COMPUTER VISION, GRAPHICS, AND IMAGE PROCESSING 48, 230–245 (1989)

NOTE

Optimal Corner Detector*

KRISHNAN RANGARAJAN, MUBARAK SHAH, AND DAVID VAN BRACKLE

Computer Science Department, University of Central Florida, Orlando, Florida 32816

Received April 27, 1988; accepted February 9, 1989

A corner is defined as the junction point of two or more straight line edges. Corners are special features in a image. They are of great use in computing the optical flow and structure from motion. In this paper, we report an optimal corner detector which uses a mathematical model for a corner. An optimal gray tone corner detector is derived for a restricted case of corners, i.e., corners made by lines which are symmetric about a horizontal axis. The resultant corner detector is described by the product of the sine in x and an exponential in the y direction in a portion of the mask and by the product of two sines in x and y directions in the remaining portion. It is then generalized to include any corner of an arbitrary angle and orientation. This results in an approximation of all corners by a total of twelve major types. It is observed that all the twelve masks can actually be configured with four smaller sub-masks, and this results in a significant reduction in the computations. The computations are further reduced by using the separability of masks. Results for synthetic and real scenes are reported.

1. INTRODUCTION

A corner is defined as the junction point of two or more straight line edges. Corners are special features in a image. They are of great use in computing the optical flow and structure from motion. In this paper, we report an optimal corner detector which uses a mathematical model for a corner. The work done by Canny [1] on edge detection has been the motivation for this work. The earliest corner detection methods involved first segmenting the image into regions and representing the object boundary as a chain code. Corners were identified where the direction changed rapidly [8]. Later attempts were directed at coming up with a corner detector which operated directly on gray level images. These include the one developed by Zuniga and Haralick [10], Kitchen and Rosenfeld [5], and the one by Dreschler and Nagel [2]. In these approaches corners are considered as the points where the rate of change of gradient direction is maximum.

We have noticed that the current corner detectors involve many stages: One has to identify edges, compute gradient direction and its rate of change, and finally apply a threshold to the rate of change of the gradient angle. Therefore, the errors occurring in any one of these stages result in poor quality corners. We have designed a new corner operator which will overcome the problems in the previous detectors.

We model the local gray level function around a corner point with additive Gaussian noise and attempt to find an optimal function representing the corner detector which when convolved with the gray level function yields a maximum at

*The research reported in this paper was supported by the Center for Research in Electro Optics and Lasers (CREOL) University of Central Florida under grant number 20-52-043 and by the National Science Foundation under grant number IRI 87-13120. A short version of this paper also appears in "Proceedings of International Conference on Computer Vision, December 1988."

0734-189X/89 $3.00

the corner point. We formulate our problem as an optimization problem and use variational calculus to solve it. In order to choose an optimal function for the desired corner detector from a class of possible functions we maximize an expression representing the performance measures of the corner detector. The resultant corner detector is described by the product of the sine in x and an exponential in the y direction in a portion of the mask and by the product of two sines in x and y directions in the remaining portion. We classify the corners into twelve types and extend the solution obtained for a restricted class of corners. We have included some additional constraints to improve the performance of the corner detector.

Our experimental results reveal that the proposed corner detector performs very well with the synthetic images with additive noise as well as the complex real images. Moreover, the computational cost of our method is $5n + 5$, where n is the mask size, which is quite low as compared to other methods reported in the literature.

Even though we have followed Canny's approach in formulating our optimization problem, our contribution is significantly different from Canny. We have contributed in developing a model of a corner and solving the equations by introducing some heuristics about the corner. Further, we have also contributed in generalizing the corner model by approximating all possible corner types with only a small number of masks, which is more crucial in the case of corners as compared to edges. Finally, we have also contributed by reducing the computation time by a significant factor.

In the next section, the related work in corner detection is reviewed briefly. The precise statement of the problem solved in this paper is given in Section 3, where we present a mathematical model of a corner having a fixed angle and a fixed orientation, and identify the performance measures of the desired corner detector. The problem of finding an optimal corner detector for a given model is formulated as an optimization problem and solved using variational calculus in Section 4. We have used some intuitive ideas to choose the unknown constants appearing in the solution. Section 5 is devoted to generalization of the corner model, while the issues related to reducing the computations are dealt with in Section 6. The algorithm is summarized in Section 7, while experimental results for synthetic and real scenes are reported in Section 8.

2. RELATED WORK

Zuniga and Haralick [10] have proposed three different methods for detecting a corner. They fit a continuous surface over a small neighborhood of each point and consider the following three quantities as measures of cornerness: 1. incremental change in gradient direction along the tangent line at the edge point; 2. incremental change in gradient direction along the contour line of the fitted surface; 3. instantaneous rate of change in gradient direction in the direction of the tangent line. Kitchen and Rosenfeld [5] have proposed three other methods to capture corners. They include: 1. Use the product of gradient of intensity and gradient of gradient direction at a pixel as a measure of cornerness. 2. Use the difference between the gradient directions of neighboring pixels which are perpendicular to the gradient direction of the pixel as a measure of its cornerness. 3. In a 3 by 3 neighborhood, locate the two pixels, A, B which are similar in gray value to the center pixel C. The difference in direction between vectors AC and CB is a measure of curvature and

hence of cornerness. Shah and Jain [9] have proposed a time varying corner detector, in which they consider the product of cornerness using facet model [10] and temporal derivative of pixel values as a basis for selecting time varying corners. Besides corners, researchers have also used other properties to choose feature points in the gray level images. One such, defined by Moravec [6], is called an *interest operator*. This calculates the sum of squared differences of adjacent pixels in the horizontal, vertical, and the two diagonal directions. Points with a local maximum for the smallest value of these four sums are used as feature points. Another feature point selection criteria is laid by Enkelmann *et al.* [3]. They classify each pixel into one of the eight bins 0 through 8, depending on the number of pixels in a 3 by 3 neighborhood having gray levels less than the central pixel.

Our approach is different from the previous approaches in the sense that we do not consider the rate of change of gradient angle for identifying corners, instead we consider the gray level characteristics around a small neighborhood of a corner having a fixed angle and orientation. We apply a corner mask to the image which responds with a very high value at the candidate corner points. Since there can only be a finite number of possible angles and orientations of corners in a digitized image, we are able to capture almost all possible corners by applying only twelve masks. The proposed corner detector is very similar in spirit to a number of edge detection schemes proposed in the literature. In these methods the edges are detected by applying a convolution mask to the image with a minimum control strategy, in some cases these edge detectors have been called edge operators in the literature. In this paper, we will also use the terms corner detector and corner operator interchangeably.

3. STATEMENT OF PROBLEM

Consider a corner at the origin oriented so that the X-axis bisects the angle as shown in Fig. 1. Let m be the slope of the upper bounding edge, and $-m$ the slope of the lower bounding edge. The function describing the gray levels around a corner is

$$I(x, y) = \begin{cases} A & \text{if } x > 0 \text{ and } -mx < y < mx \\ 0 & \text{otherwise.} \end{cases}$$

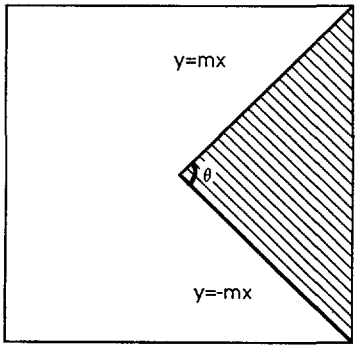

FIG. 1. A corner model.

Let $g(x, y)$ be the operator to be determined, and $n(x, y)$ be white Gaussian noise. Then the gray level function with the additive noise is

$$F(x, y) = I(x, y) + n(x, y).$$

We are interested in detecting a corner at the origin by first convolving $F(x, y)$ with an unknown function $g(x, y)$ called a corner operator and then identifying the maximum of the result, $O(x, y) = F(x, y) * (x, y)$, where " $*$ " is the convolution operation. There will be a class of functions containing $g(x, y)$ which will satisfy the above requirement, but we want to pick the function which best fulfills the following criteria: 1. The operator should not be sensitive to the noise. 2. It should not delocalize corner points. 3. The detected corner point should also be an edge point. 4. The detected corner point should have at least two neighbors which have a different gradient direction than the corner point itself. The above criteria guarantee elimination of false corners and detection of valid localized corners. They also enforce the intuitive notion that a corner is the intersection of two physical edges. We have been able to convert the first two qualitative criteria into quantitative functions. We will use signal to noise ratio (SNR) to represent the first criteria and $E[x_0^2 + y_0^2]$ for delocalization, where E is the expectation operator and (x_0, y_0) is the location where the corner at $(0, 0)$ is actually detected. Criteria (3) and (4) will be enforced by removing candidate points which are not edge points and by removing candidate corner points which contain two edge points having the same gradient angle in a small neighborhood.

4. FINDING OPTIMAL CORNER DETECTOR

In this section we formulate the problem of finding a corner detector as an optimization problem and solve it using variational calculus. In our case, the corresponding Euler equation gives rise to two differential equations which are solved in Section 4.2 while the unknown constants are chosen in Section 4.3.

4.1. *Formulation of Optimization Problem*

Our aim is to find an *optimal corner detector* which will satisfy the criteria listed in the previous section. We will use optimization techniques to find an expression for $g(x, y)$ such that a performance measure Σ is maximized. We will follow Canny [1] and use *SNR* (Ξ) and *Delocalization* (Λ) as performance measures for our corner detector. The signal to noise ratio and the delocalization terms can be derived to be the following expressions:

$$\Xi = \frac{A\int_0^{+\infty}\int_{-mx}^{+mx} g(x, y)\, dy\, dx}{n_0\sqrt{\int_{-\infty}^{+\infty}\int_{-\infty}^{+\infty} g^2(x, y)\, dy\, dx}} \tag{1}$$

$$\Lambda = \frac{n_0^2\int_{-\infty}^{+\infty}\int_{-\infty}^{+\infty} g_x^2(x, y)\, dy\, dx}{\left(A\int_0^{+\infty}\int_{-mx}^{+mx} g_{xx}(x, y)\, dy\, dx\right)^2} + \frac{n_0^2\int_{-\infty}^{+\infty}\int_{-\infty}^{+\infty} g_y^2(x, y)\, dy\, dx}{\left(A\int_0^{+\infty}\int_{-mx}^{+mx} g_{yy}(x, y)\, dy\, dx\right)^2}, \tag{2}$$

where n_0^2 is the variance of the Gaussian $n(x, y)$, g the operator to be determined, g_x, g_y, g_{xx}, g_{yy} the partial derivatives of g, A the contrast of the corner, and m the slope of the bounding edges in the corner model. For an ideal corner detector one will be interested in *zero* delocalization and very *high* value of signal to noise ratio. Therefore, we will use the quotient of Ξ and Λ) as given below as the expression we want to maximize,

$$\Sigma = \frac{\dfrac{A\displaystyle\int_0^{+\infty}\int_{-mx}^{+mx} g(x, y)\, dy\, dx}{n_0\sqrt{\displaystyle\int_{-\infty}^{+\infty}\int_{-\infty}^{+\infty} g^2(x, y)\, dy\, dx}}}{\dfrac{n_0^2\displaystyle\int_{-\infty}^{+\infty}\int_{-\infty}^{+\infty} g_x^2(x, y)\, dy\, dx}{\left(A\displaystyle\int_0^{+\infty}\int_{-mx}^{+mx} g_{xx}(x, y)\, dy\, dx\right)^2} + \dfrac{n_0^2\displaystyle\int_{-\infty}^{+\infty}\int_{-\infty}^{+\infty} g_y^2(x, y)\, dy\, dx}{\left(A\displaystyle\int_0^{+\infty}\int_{-mx}^{+mx} g_{yy}(x, y)\, dy\, dx\right)^2}}. \quad (3)$$

The general strategy is to use the calculus of variations to maximize (or minimize) one of the integrals with the others held constant. However, the fact that the integrals have different limits cannot be handled easily in the calculus of variations. Therefore, we need to change the finite limits into infinite limits. Our method is to let $H(x, y)$ be a function defined as follows:

$$H(x, y) = \begin{cases} 1 & \text{if } x > 0 \text{ and } -mx < y < mx \\ 0 & \text{otherwise.} \end{cases}$$

Then, all the integrals may be given infinite limits,

$$\int_0^{+\infty}\int_{-mx}^{+mx} K(x, y)\, dy\, dx = \int_{-\infty}^{+\infty}\int_{-\infty}^{+\infty} K(x, y) H(x, y)\, dy\, dx.$$

The expression to be maximized is then

$$\Sigma = \frac{\dfrac{A\displaystyle\int_{-\infty}^{+\infty}\int_{-\infty}^{+\infty} g(x, y) H(x, y)\, dy\, dx}{n_0\sqrt{\displaystyle\int_{-\infty}^{+\infty}\int_{-\infty}^{+\infty} g^2(x, y)\, dy\, dx}}}{\dfrac{n_0^2\displaystyle\int_{-\infty}^{+\infty}\int_{-\infty}^{+\infty} g_x^2(x, y)\, dy\, dx}{\left(A\displaystyle\int_{-\infty}^{+\infty}\int_{-\infty}^{+\infty} g_{xx}(x, y) H(x, y)\, dy\, dx\right)^2} + \dfrac{n_0^2\displaystyle\int_{-\infty}^{+\infty}\int_{-\infty}^{+\infty} g_y^2(x, y)\, dy\, dx}{\left(A\displaystyle\int_{-\infty}^{+\infty}\int_{-\infty}^{+\infty} g_{yy}(x, y) H(x, y)\, dy\, dx\right)^2}}.$$

The maximization may now be stated as a variational calculus problem: minimize $\int_{-\infty}^{+\infty}\int_{-\infty}^{+\infty} g^2(x, y)\, dy\, dx$ with all other integrals held constant as constraints. Minimizing the term in the denominator and keeping all the other terms constant we will essentially maximize the above expression. Refer to Appendix A in [4] for introductory material on variational calculus.

4.2. *Solving for g*

With LaGrange multipliers, we can write the above problem as

$$\text{minimize} \int_{-\infty}^{+\infty}\int_{-\infty}^{+\infty} F(x, y, g, g_x, g_y, g_{xx}, g_{yy})\, dy\, dx,$$

where $F(x, y, g, g_x, g_y, g_{xx}, g_{yy}) = g^2 + \lambda_1 Hg + \lambda_2 g_x^2 + \lambda_3 g_y^2 + \lambda_4 Hg_{xx} + \lambda_5 Hg_{yy}$. The related Euler equation is given by

$$F_g - \frac{\partial}{\partial x}F_{g_x} - \frac{\partial}{\partial y}F_{g_y} + \frac{\partial^2}{\partial x^2}F_{g_{xx}} + \frac{\partial^2}{\partial y^2}F_{g_{yy}} = 0.$$

Taking the partial differentials of F and substituting their values in the above equation we get

$$2g + \lambda_1 H - 2\lambda_2 g_{xx} - 2\lambda_3 g_{yy} + \lambda_4 \frac{\partial^2}{\partial x^2}H + \lambda_5 \frac{\partial^2}{\partial y^2}H = 0.$$

Since $H(x, y)$ is constant, its derivatives are zero; therefore the last two terms in the above equation will disappear. Now, setting $\lambda_1/2 = \mu$, the above equation becomes

$$\lambda_2 g_{xx} + \lambda_3 g_{yy} - g = \mu H.$$

Since $H(x, y) = 1$ when $x < 0$ and $-mx < y < mx$, thus, it is necessary to solve two differential equations:

$$\lambda_2 g_{xx} + \lambda_3 g_{yy} - g = \mu \qquad \text{when } x > 0,\ -mx < y < mx \tag{4}$$

$$\lambda_2 g_{xx} + \lambda_3 g_{yy} - g = 0 \qquad \text{otherwise.} \tag{5}$$

Let us call the part of function $g(x, y)$ defined by Eq. (4) as the *cone portion* of the mask and that defined by Eq. (5) as the *non-cone portion* of the mask.

Solving Eqs. (4) and (5) by separation of variables [7], we get

$$g(x, y) = c_1 \sin\frac{m\pi x}{W}\left[-\left(e^{zW} + e^{-zW}\right) + e^{zy} + e^{-zy}\right] \tag{6}$$

$$g(x, y) = c_2 \sin\frac{n_1\pi x}{W}\sin\frac{n_2\pi y}{W}, \tag{7}$$

where W is the mask size, and c_1, c_2, m, n_1, n_2, and z are constants. The cone portion of the mask is formed by Eq. (6) and the non-cone portion is formed by Eq. (7).

4.3. *Choosing Unknown Constants*

Our optimal corner detector is described by two equations: Equation (6) is applicable to the cone portion of the mask and Eq. (7) applicable to the non-cone portion of the mask. The constants c_1 and c_2 can be set to 1 as they are going to just scale the values in the mask. These two solutions involve four other unknown constants:

- m found in the sine term, $\sin(m\pi x/W)$ in both the solutions for cone portion.
- n_1 found in the sine term, $\sin(n_1\pi x/W)$ in the solution for non-cone portion.
- n_2 found in the sine term, $\sin(n_2\pi x/W)$ found in the solution for the non-cone portion.
- z found in the exponential term in the solution for the cone portion.

In this section, we develop some rationale for selecting the values of these four unknowns. Since the image is discrete we would like to come up with a discrete mask for our optimal corner detector described by Eqs. (6) and (7). This will be achieved by sampling the continuous functions at integer values for x and y.

A mask for detecting a corner formed by lines symmetric about the horizontal axis can be developed based on the following intuitive ideas. As usual, we will assume that the gray levels corresponding to the object are higher than the background. Let us stick to the ideal case in which there is no noise. The distinction of the corner pixel over the bright image pixels is that it has the maximum number of background pixels as its neighbor. So if we apply a corner mask, which has negative weights in the non-cone portion and positive weights in the cone portion, the corner pixel will stand out giving a very high value in the result.

Now, let us attempt to determine the value of the first unknown m. It is to be noted that the term $[-(e^{zW} + e^{-zW}) + e^{zy} + e^{-zy}]$ in Eq. (6) is always negative, as $0 \le y \le W$ in the cone portion. When $m = -1$, for x varying from 0 to W, the $\sin(m\pi x/W)$ term varies from $\sin 0$ to $\sin -\pi$ which is then one-half of the sine wave having negative values. If m takes any other value, some negative values will appear in the cone portion which is not desired. The intuitive mask has negative values in the non-cone portion. To achieve this for the optimal mask we choose $n_1 = 1$ and $n_2 = -1$, thus the $\sin(n_2\pi x/W)$ term is out of phase by 180° with $\sin(n_1\pi x/W)$ and the product in Eq. (7) is always negative. We have not been able

-3	-5	-5	-3	0	-3	-5	-5	-3
-5	-9	-9	-5	0	-5	-9	-9	-5
-5	-9	-9	-5	0	-5	-9	8	5
-3	-5	-5	-3	0	6	9	9	6
0	0	0	0	0	6	10	10	6
-3	-5	-5	-3	0	6	9	9	6
-5	-9	-9	-5	0	-5	-9	8	5
-5	-9	-9	-5	0	-5	-9	-9	-5
-3	-5	-5	-3	0	-3	-5	-5	-3

FIG. 2. Optimal masks for 60°.

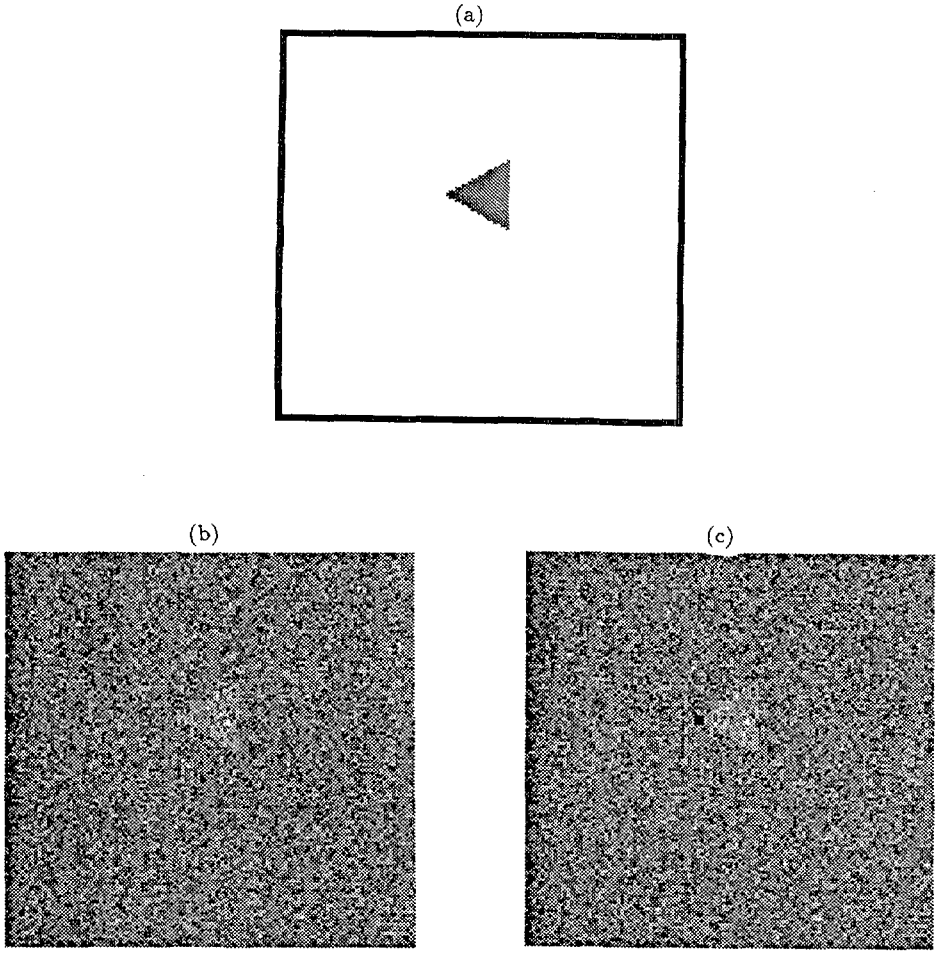

FIG. 3. Results of optimal corner detector for a noisy image: (a) synthetic image of 60°; (b) synthetic image with additive Gaussian noise of $\sigma = 4$; (c) detected corner superposed on the original image.

to find any rationale for selecting the value of z yet; however, we have noted from our experiments that the higher the value of z the greater is the noise fighting capability of the mask. One could also vary the size of the mask ($2W$) and as it is clear from Eq. (6) this will have similar effect on performance of corner detector as of z.

The optimal mask of size 9 by 9 was created for $\theta = 60°$, with $m = -1$, $n_1 = 1$, $n_2 = -1$, and $z = 0.2$ and is shown in Fig. 2. The masks were applied to the test cases listed previously without noise and with an additive noise of $\sigma = 64$. A sample of the results is shown in the Fig. 3.

5. GENERALIZING THE MODEL

So far our model for a corner has been very simple and unrealistic. We have assumed that the corner is made by lines symmetric about the x axis. This implies

that the orientation of the corner is fixed. But in a real image the corner can appear in any arbitrary orientation. Also, another restriction in our model is that the mask is dependent on the slope of the lines making the corner, which would mean a large number of masks to cover all the possible slopes of lines.

It would be very hard to enumerate all possible corners and generate a mask for each one of them. One can attempt to come up with a small class of corners which can approximate most of the possible corners in real images. We have found that there are three major classes of corners depending on the total number of quadrants occupied by the cone portion of the corner in our model. The first class contains all the corners in which the cone portion lies in only one quadrant; the second class contains all the corners in which the cone portion lies in two consecutive quadrants; finally the third class contains all the corners in which the cone portion lies in three consecutive quadrants. Therefore, in total we have 13 corner types as shown in

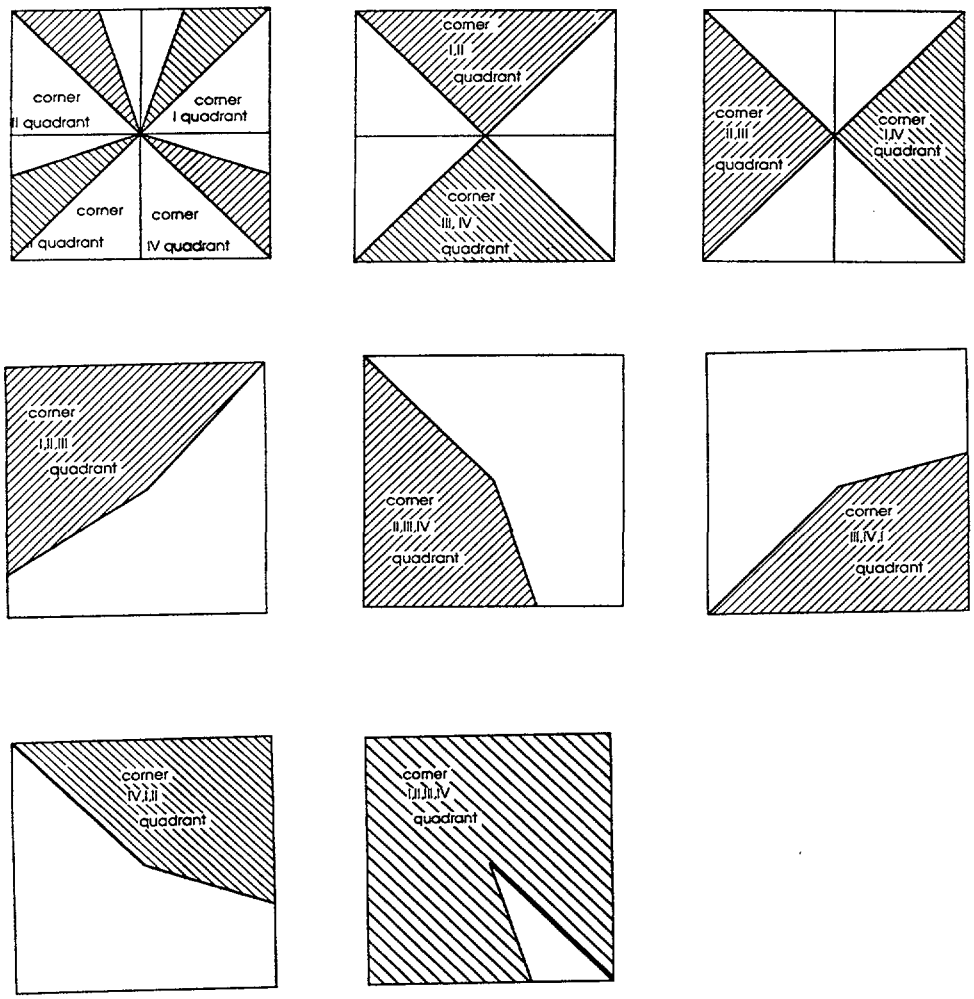

FIG. 4. Types of corners.

-6	-11	-11	-6	0	4	7	7	4
-11	-18	-18	-11	0	8	13	13	8
-11	-18	-18	-11	0	10	17	17	10
-6	-11	-11	-6	0	12	19	19	12
0	0	0	0	0	12	20	20	12
-6	-11	-11	-6	0	-6	-11	-11	-6
-11	-18	-18	-11	0	-11	-18	-18	-11
-11	-18	-18	-11	0	-11	-18	-18	-11
-6	-11	-11	-6	0	-6	-11	-11	-6

FIG. 5. Approximate optimal mask.

Fig. 4. One of these types in which the cone portion will occupy all four quadrants, while the non-cone portion will not be present at all and will violate our corner model. We propose to use only 12 masks to detect any corner having an arbitrary angle and orientation.

For each of the cases listed above the mask is formed as follows. Use the solution given in Eq. (6) for the quadrant(s) containing the cone portion of the corner and the solution given in Eq. (7) for the remaining quadrants. For example, in Fig. 5 we have shown a mask generated by this method for detecting corners with the cone portion in quadrant I. Note that this mask is ideal for detecting corners which make 90° with the X-axis. However, this mask will respond to almost all the possible corners in quadrant I. The difference between the ideal corner of 90° and any other corner in quadrant I is that in the former case the cone portion will occupy the whole quadrant, while in the latter case the cone portion will occupy only a part of quadrant I depending on the angle of the corner. Therefore, the total response of the mask at the corner point in the ideal case will be higher than the response of the mask for any other angle. Recall that this observation is true for the previous approaches also; in these approaches the rate of change of gradient angle is used as the measure of cornerness. The rate of change is higher for the ideal case of 90° as compared to the rate of change of any smaller angle.

4	7	7	4	0
8	13	13	8	0
10	17	17	10	0
12	19	19	12	0
0	0	0	0	0

(a)

12	19	19	12	0
10	17	17	10	0
8	13	13	8	0
4	7	7	4	0
0	0	0	0	0

(b)

-6	-11	-11	-6	0
-11	-18	-18	-11	0
-11	-18	-18	-11	0
-6	-11	-11	-6	0
0	0	0	0	0

(c)

12	20	20	12	0

(d)

FIG. 6. Four principal sub-masks: (a) $C1$; (b) $C2$; (c) NC; (d) CX.

6. REDUCING COMPUTATIONS

In the previous section, we found that a total of 12 masks will be needed to detect a corner of any angle appearing in an arbitrary orientation. For a mask of size 11, the 12 masks will require 11*11*12 multiplications for each pixel in an image. Computationally this method will be very expensive. It can be observed that each of the twelve masks can be constructed from the four submasks shown in Fig. 6. As an example, Fig. 7 shows how the mask for corner Type-1 is constructed from these four sub-masks. Let $I(x, y)$ be the image value at point (x, y) and let $(2n + 1)$ be the mask size. Let us compute the following values at each pixel (x, y).

$$I_{C1}(x, y) = I * C1(x, y) = \sum_{j=-n/2}^{n/2} \sum_{i=0}^{n} C1(i, j) \cdot I(x + i, y + j)$$

$$I_{C2}(x, y) = I * C2(x, y) = \sum_{j=0}^{n} \sum_{i=0}^{n} C2(i, j) \cdot I(x + i, y + j)$$

$$I_{NC}(x, y) = I * NC(x, y) = \sum_{j=0}^{n} \sum_{i=0}^{n} NC(i, j) \cdot I(x + i, y + j)$$

$$I_{CX}(x, y) I * CX(x, y) = \sum_{j=0}^{n} CX(i, j) \cdot I(x, y + j).$$

Now, $I(x, y) * g(x, y)$ for corner Type-1 can be computed as

$$\begin{aligned} I(x, y) * g(x, y) = {} & I_{C1}(x + d, y + d - 1) + I_{CX}(x + d, y) \\ & + I_{NC}(x + d, y - d) + I_{NC}(x - d + 1, y + d - 1) \\ & + I_{NC}(x - d + 1, y - d), \end{aligned}$$

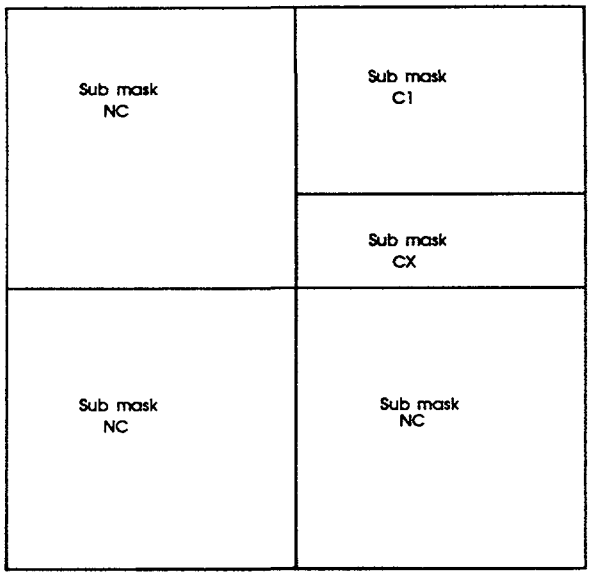

FIG. 7. Generation of mask for Type-1 corner.

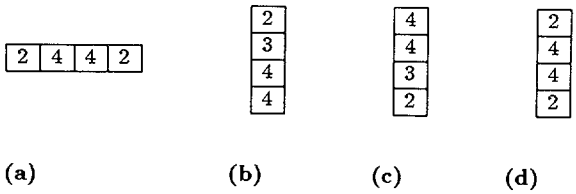

FIG. 8. One-dimensional masks using separability: (a) $XC1$; (b) $YC1$; (c) $YC2$; (d) $YC3$.

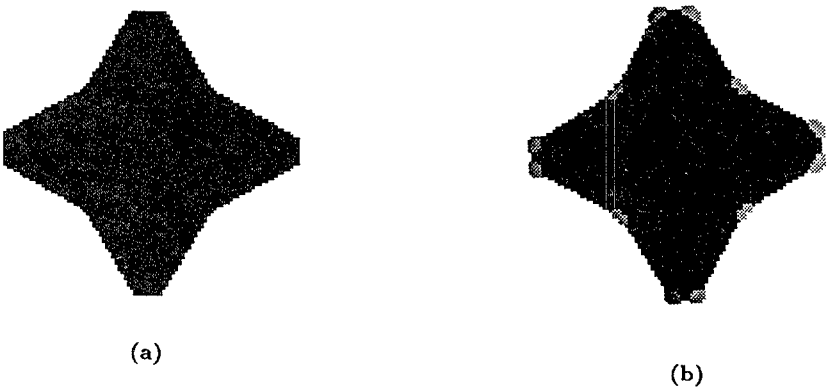

FIG. 9. Results of corner detector for the synthetic image: (a) original image; (b) detected corners superposed on the original image.

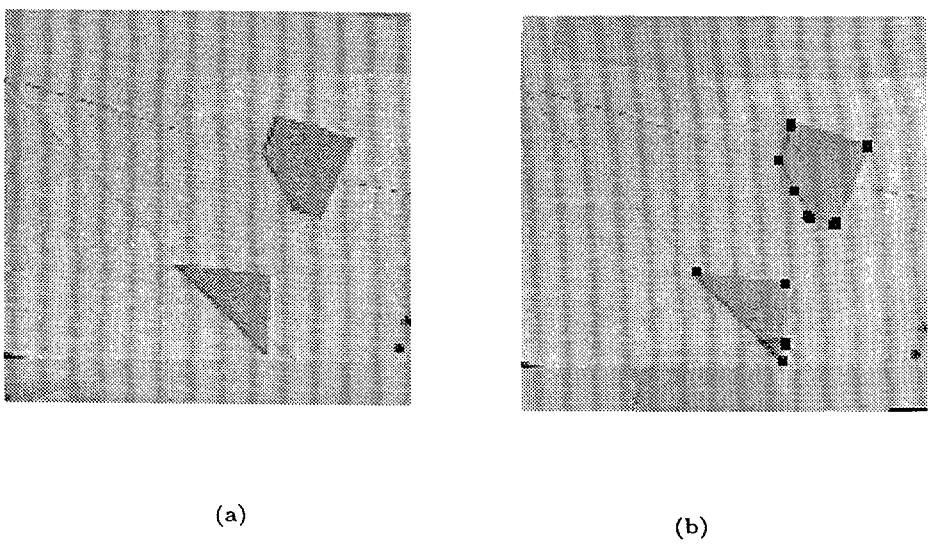

FIG. 10. Results of corner detector for the cardboard image: (a) original image; (b) detected corners superposed on the original image.

where $d = \frac{1}{2}(n + 1)$. Since all 12 masks can be constructed from the sub-masks $C1$, $C2$, NC, and CX, it is sufficient to compute $I * C1(x, y)$, $I * C2(x, y)$, $I * NC(x, y)$, $I * CX(x, y)$ for each pixel (x, y) in the image and combine these results to get all of the 12 masks.

Further, sub-masks $C1$, $C2$, and NC can be split into two one-dimensional masks. For example, $C1$ is split into $XC1$ and $YC1$, $XC1$ using solution (6) and $YC1$ using solution (7) (Fig. 8). Now the operation $I(x, y) * C1(x, y)$ can be computed as

$$I(x, y) * C1(x, y) = \left(\sum_{j=0}^{n} \left(\sum_{i=0}^{n} I(x + i, y + j) \cdot XC1(i) \right) \cdot YC1(j) \right).$$

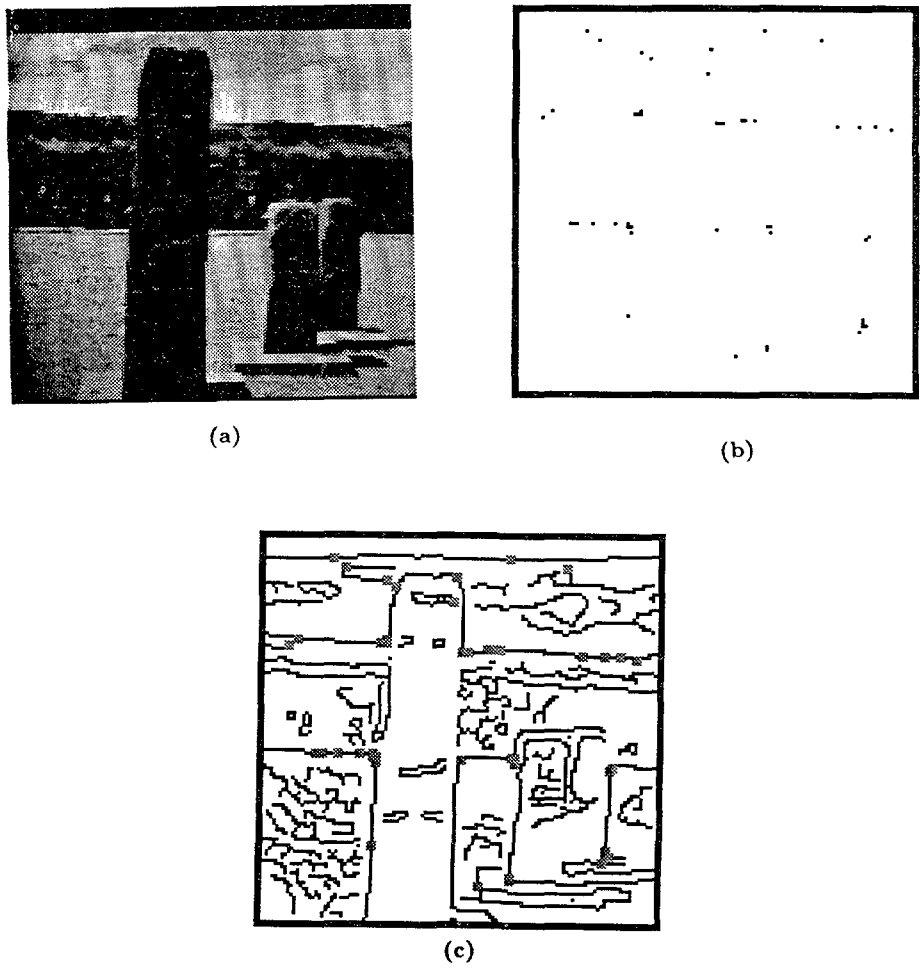

FIG. 11. Results of corner detector for the Tiwanaku image: (a) original image; (b) detected corners; (c) detected corners superposed on the edge image.

The computational cost of our method is $5n + 5$, where n is the mask size. Which is quite low as compared to other methods reported in the literature. Moreover, our method gives superior results.

7. SUMMARY OF ALGORITHM

In this section, we describe the final algorithm for detecting corners. For each of the 12 masks perform the following steps:

1. Compute cornerness at all pixels by applying the corner masks to the given image.

2. Select the pixels with value greater than a preset global threshold as candidate corners. Typically a low threshold like 50% of the maximum response is

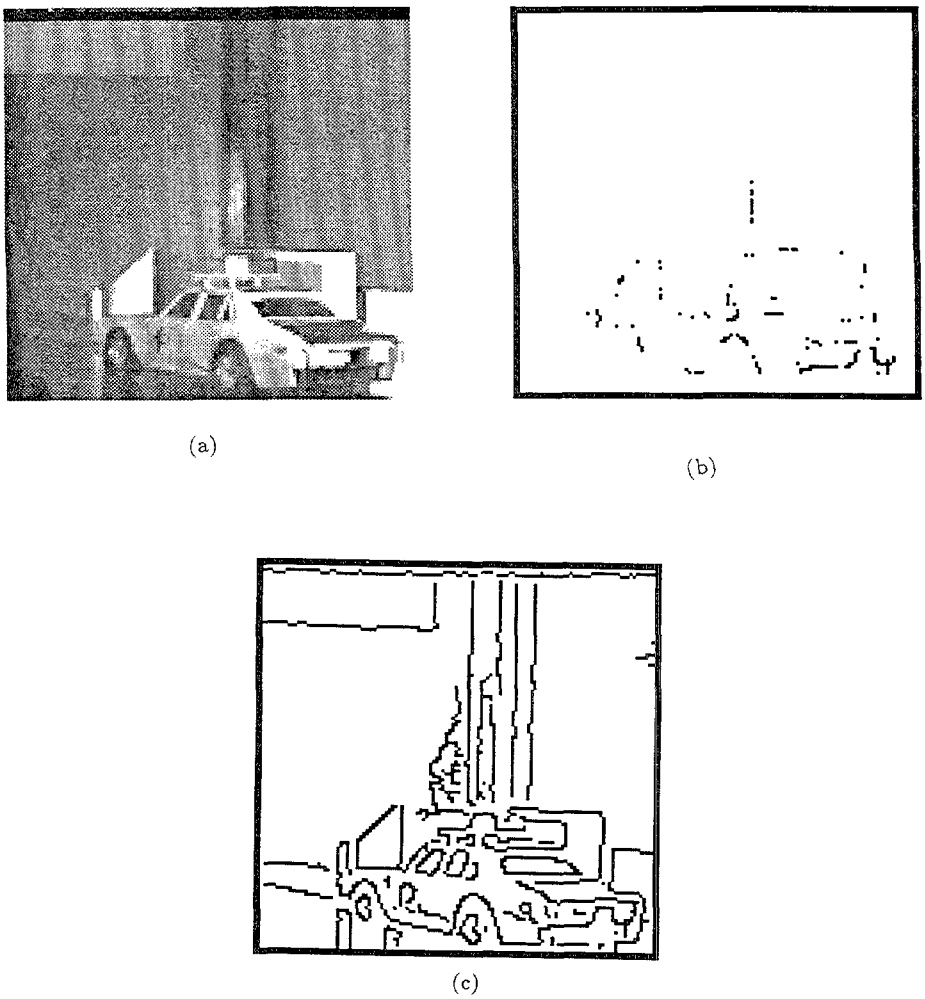

FIG. 12. Results of corner detector for the car image: (a) original image; (b) detected corners; (c) edge image.

used to retain all corners, and the later steps are used for eliminating noncorner points.

3. As a corner pixel is also an edge pixel, remove candidate corner pixels obtained from the previous step that are not edge pixels. We use Canny's operator for finding the edge pixels.

4. Discard corners which have at least two neighbors in a 3 by 3 neighborhood with a similar gradient angle.

5. Declare the remaining corners as valid corners.

8. EXPERIMENTAL RESULTS

Figures 9-12 show the results obtained using our corner detector for some synthetic and real images. In Fig. 9a a synthetic image of corners of 120° and 210° are shown, while Fig. 9b shows the original image with the superposed corners detected by our method. Next, the results for a real scene of two objects are shown in Figs. 10a, b. This image is taken from a cardboard sequence of moving objects. Notice that all true corners are detected; in addition, one false corner is also detected in the lower object. In fact, this additional corner is a valid corner which is made between the lower object and a thin edge running through the object. Next, Figs. 11a–c show the results obtained for the Tiwanaku image. Notice that this is a very complex image with lots of potential corners. However, our corner detector is able to identify most true corners in two standing statues. Finally, the results for a toy car are shown in Figs. 12a–c.

9. CONCLUSIONS

We have presented a new approach for modelling a corner in gray level images, which is significantly different from the previous approaches which model a corner as a point where the rate of change of gradient angle is high. Using this new mathematical model we derived an optimum corner detector which, when convolved with the gray level image, responds with a very high value at the location of the corner. We have shown by presenting the experimental results for the synthetic and real scenes that the performance of our corner detector is very good. Further, we have outlined a very efficient algorithm which uses the separability of corner masks to reduce the computational cost. Our future work will focus on the use of corners as tokens for establishing correspondence in a sequence of frames.

ACKNOWLEDGMENT

The authors are thankful to Donna Williams for her valuable comments and suggestions on the earlier drafts of this paper.

REFERENCES

1. J. F. Canny, *Finding Edges and Lines in Images*, Master's thesis, MIT, 1983.
2. L. Drechler and H. Nagel, Volumetric model and 3-d trajectory of a moving car derived from monocular tv-frame sequence of a street scene, in *Proceedings, IJCAI, 1981*, pp. 692–697.
3. W. Enkelmann, R. Kories, H. H. Nagel, and G. Zimmermann, *An Experimental Investigation of Estimation Approaches for Optical Flow Fields*, technical report, Fraunhofer-Institut fur Informations und Datenverarbeitung Sebastian Kneipp Strabe 12-14 7500 Karlsruhe 1/FR Germany, 1987.
4. B. K. P. Horn, *Robot Vision*, MIT Press, Cambridge, MA, 1986.
5. L. Kitchen and A. Rosenfeld, Edge evaluation using local edge coherence, *IEEE Trans. Systems Man Cybernet.* **SMC-11**, No. 9, 1981, 597–605.

6. H. P. Moravec, Towards automatic visual obstacle avoidance, in *IJCAI-5, 1977.*
7. K. Rangaraj, M. Shah, and D. Van Brackle, *Optimal Corner Detector*, technical report CS-TR-11-88, University of Central Florida, Computer Science Department, May 1988.
8. W. S. Rutkowski and R. Rosenfeld, *A Comparison of Corner Detection Techniques for Chain Coded Curves*, technical report No. 263, University of Maryland, 1977.
9. M. Shah and R. Jain, *Time-Varying Corner Detector*, technical report CRL-TR-34-83, University of Michigan Computing Research Laboratory, December 1983.
10. O. A. Zuniga and R. Haralick, Corner detection using the facet model, in *IEEE CVPR, 1983*, pp. 30–37.